

# **Rhodopsin Photoisomerization: Coherent vs. Incoherent Excitation**

Kunihito Hoki and Paul Brumer

*Chemical Physics Theory Group, Department of Chemistry,  
and Center for Quantum Information and Quantum Control,*

*University of Toronto, Toronto, Canada M5S 3H6*

(Dated: May 4, 2006)

## **Abstract**

A uniform minimal model of rhodopsin photoisomerization induced by either coherent laser light or low level incoherent light (e.g. moonlight) is provided. Realistic timescales for both processes, which differ by ten orders of magnitude, are obtained. Further, a kinetic scheme involving rates for both coherent and incoherent light excitation is introduced, placing all timescales into a uniform framework.

**Keyword:** rhodopsin, isomerization, femtosecond laser, incoherent light

## I. INTRODUCTION

Developments in fast pulsed lasers have allowed for the detailed study of photobiological processes such as laser induced *cis/trans* isomerization of rhodopsin, a process of interest due to the large quantum yield ( $\sim 65\%$ ), high speed ( $\sim 200$  fs) of reaction, and importance in the function of living organisms [1, 2, 3]. However, photoinduced processes such as this occur naturally in the presence of weak incoherent light, rather than in the strong coherent light that emanates from laser sources. For example, photoabsorption in rhodopsin initiates vertebrate visual transduction in dim light, such as moonlight [4]. Since the processes induced by these two types of sources are qualitatively different, e.g. pulsed coherent light induces time dependent molecular dynamics, whereas purely incoherent light does not [5, 6], it is important to establish the relationship between them.

In this paper, we provide a uniform minimal model for photoisomerization induced by either of these light sources and demonstrate: (a) a computed dynamics timescale for femtosecond laser pulse excitation in agreement with experiment, (b) realistic dynamics for time scales on the order of milliseconds for moonlight induced processes, and (c) a kinetic scheme involving rates of both incoherent and coherent excitation that places all timescales within a unified framework. Specifically, in the natural visual process, the femtosecond coherent timescales provide the initial rise of the *cis/trans* isomerization and the millisecond incoherent timescale gives the rate of the process at longer times.

## II. THEORY

Our theoretical treatment of the photoisomerization is based on a one dimensional system with two electronic states (see Fig. 1a) connecting the *cis* and *trans* configurations, coupled through a strength parameter  $\eta$  to a “bath” that models the effects of the remaining degrees of freedom and of the external environment. Isomerization occurs via rotation about an angle  $\alpha$ . The interaction potential between the system and the coherent external field  $E(t)$  is treated by means of the dipole approximation. In the case of low level incoherent light,  $E(t) = 0$  and a second bath describing the incoherent light is included. That is, our Hamiltonian is

$$H_T = H_S - \mu E(t) + H_{\text{Ienv}} + H_{\text{env}} + H_{\text{Irad}} + H_{\text{rad}}, \quad (1)$$

where  $H_S$  is system Hamiltonian,  $\mu$  is transition dipole moment of the system,  $E(t)$  is electric field of the laser pulse,  $H_{\text{env}}$  is the environment Hamiltonian,  $H_{\text{Ienv}}$  is the interaction Hamiltonian between the system and environment,  $H_{\text{rad}}$  describes blackbody radiation, and  $H_{\text{Irad}}$  is interaction Hamiltonian between the system and the radiation field. Eigenstates  $|i\rangle$  of the system  $H_S$  satisfy

$$H_S |i\rangle = \lambda_i |i\rangle, \quad (2)$$

and the density matrix accounted with evolution of the (system + bath) is denoted  $\rho_T$ . The system density matrix is  $\rho = \text{Tr}_B \rho_T$ , where  $\text{Tr}_B$  denotes a trace over the bath. The time propagation of the density matrix elements of the system  $\rho_{ij}(t) = \langle i | \rho(t) | j \rangle$  is described by

Redfield theory within a secular approximation [7, 8, 9, 10] as,

$$\begin{aligned} \frac{\partial}{\partial t} \rho_{ii} = & \sum_{j \neq i} w_{ij} \rho_{jj} - \rho_{ii} \sum_{j \neq i} w_{ji} \\ & - i \frac{E(t)}{\hbar} \sum_m [\rho_{im}(t) \mu_{mi} - \mu_{im} \rho_{mi}(t)] \end{aligned} \quad (3)$$

$$\begin{aligned} \frac{\partial}{\partial t} \rho_{ij} = & -i\omega_{ij} \rho_{ij}(t) - \gamma_{ij} \rho_{ij}(t) \\ & - i \frac{E(t)}{\hbar} \sum_m [\rho_{im}(t) \mu_{mj} - \mu_{im} \rho_{mj}(t)] \quad (i \neq j), \end{aligned} \quad (4)$$

where  $w_{ji} = \Gamma_{ijji}^+ + \Gamma_{ijji}^-$  is transition probability per unit time from  $i$ th to  $j$ th eigen state of  $H_S$ , and  $\gamma_{ij} = \sum_k (\Gamma_{ikki}^+ + \Gamma_{jkkj}^-) - \Gamma_{jjii}^+ - \Gamma_{jjii}^-$  is dephasing rate. Here,

$$\begin{aligned} \Gamma_{ljik}^+ = & \frac{1}{\hbar^2} \int_0^\infty d\tau e^{-i\omega_{ik}\tau} \langle H_{\text{Ienv}_{lj}}(\tau) H_{\text{Ienv}_{ik}} \rangle_{\text{env}} \\ & + \frac{1}{\hbar^2} \int_0^\infty d\tau e^{-i\omega_{ik}\tau} \langle H_{\text{Irad}_{lj}}(\tau) H_{\text{Irad}_{ik}} \rangle_{\text{rad}} \end{aligned} \quad (5)$$

$$\Gamma_{ljik}^- = (\Gamma_{kijl}^+)^*, \quad (6)$$

where the brackets  $\langle \dots \rangle_B$  represent a trace over degrees of freedom in B, where B is either the environment “env” or the incoherent radiation field “rad”, and  $H_{IB}(t) = e^{iH_B t/\hbar} H_{IB} e^{-iH_B t/\hbar}$ .

The system Hamiltonian  $H_S$  is given in terms of two diabatic electronic states by

$$H_S = \begin{pmatrix} T + V_g(\alpha) & V_{ge}(\alpha) \\ V_{eg}(\alpha) & T + V_e(\alpha) \end{pmatrix}, \quad (7)$$

where  $T = -\frac{\hbar^2}{2m} \frac{\partial^2}{\partial \alpha^2}$  is the kinetic energy,  $V_g(\alpha)$  and  $V_e(\alpha)$  are the potential energy surfaces in ground and excited electronic state, and  $V_{ge}(\alpha) = V_{eg}(\alpha)$  is the coupling potential between ground and excited states (see Fig. 1a).

The environment is described as a set of harmonic oscillators of frequency  $\omega'_n$  and the system–environment coupling is  $H_{\text{Ienv}} = Q \sum_n \hbar \kappa_n (b_n^\dagger + b_n)$ , where  $b_n^\dagger$  and  $b_n$  are the creation and annihilation operators pertaining to the  $n$ th harmonic oscillator. The operator  $Q$  is a diagonal  $2 \times 2$  matrix with  $\cos \alpha$  on the diagonal, and the coupling constants  $\kappa_n$  and spectrum of the bath are chosen in accord with an Ohmic spectral density  $J(\omega) = 2\pi \sum_n \kappa_n^2 \delta(\omega - \omega'_n) = \eta \omega e^{-\omega/\omega_c}$ , where the strength of the system–environment coupling is determined by the dimensionless parameter  $\eta$ , and  $\omega_c = 300 \text{ cm}^{-1}$ . After some algebra, we obtain first term of Eq. (5) as,

$$\begin{aligned} & \frac{1}{\hbar^2} \int_0^\infty d\tau e^{-i\omega_{ik}\tau} \langle H_{\text{Ienv}_{lj}}(\tau) H_{\text{Ienv}_{ik}} \rangle_{\text{env}} \\ &= \frac{1}{2\pi} Q_{lj} Q_{ik} \int_0^\infty d\tau \int_0^\infty d\omega J(\omega) \cdot \\ & \quad \cdot \{ [\bar{n}(\omega) + 1] e^{-i(\omega_{ik} + \omega)\tau} + \bar{n}(\omega) e^{-i(\omega_{ik} - \omega)\tau} \}, \end{aligned} \quad (8)$$

where  $\bar{n}(\omega) = \{\exp(\hbar\omega/k_b T) - 1\}^{-1}$  is the Bose distribution at temperature  $T = 300 \text{ K}$ ,  $\omega_{ji} = (\lambda_j - \lambda_i)/\hbar$ , and  $\lambda_i$  is an eigenenergy of  $H_S$ .

As a typical situation of scotopic vision, we consider moonlight, which is well characterized as a blackbody source at  $4100 \text{ K}$  [11]. The radiation field is also described as a set of harmonic oscillators of frequency  $\omega''_n$  and the system–radiation field coupling is treated by means of dipole approximation as,

$$H_{\text{Irad}} = \mu \sum_{\mathbf{k}} i \sqrt{\frac{\hbar \omega''_{\mathbf{k}}}{2\epsilon_0 V}} \sin \theta \{ a_{\mathbf{k}} \exp(i\mathbf{k} \cdot \mathbf{r}) - a_{\mathbf{k}}^\dagger \exp(-i\mathbf{k} \cdot \mathbf{r}) \}, \quad (9)$$

where  $\mathbf{k}$  is a wave number vector,  $\epsilon_0$  is the permittivity of vacuum,  $\mathbf{r}$  is a position inside of

a cavity,  $V$  is volume of the cavity, and  $\theta$  is an angle between the transition dipole moment vector and  $\mathbf{k}$  [12]. By assuming the large cavity limit the summation of  $\mathbf{k}$  can be replaced with integrals, and second term of Eq. (5) is written as,

$$\begin{aligned} & \frac{1}{\hbar^2} \int_0^\infty d\tau e^{-i\omega_{ik}\tau} \langle H_{\text{Irad}_{lj}}(\tau) H_{\text{Irad}_{ik}} \rangle_{\text{rad}} \\ &= C \frac{\mu_{lj}\mu_{ik}}{2\hbar\epsilon_0\pi^3} \int_0^\infty d\tau \int_0^\infty dk \int_0^{\frac{\pi}{2}} d\theta \int_0^{\frac{\pi}{2}} d\phi k^2 \sin\theta^3 \cdot \\ & \quad \cdot \left[ (\bar{n}(\omega_k'') + 1) e^{-i(\omega_k'' + \omega_{ik})\tau} + \bar{n}(\omega_k'') e^{i(\omega_k'' - \omega_{ik})\tau} \right]. \end{aligned} \quad (10)$$

A component of the imaginary part of Eq. (10) describes the Lamb shift. The integration with respect to  $k$  does not converge, and this difficulty can be avoided by renormalization theory [13]. However, since the effect of Lamb shift is generally less than  $0.1 \text{ cm}^{-1}$ , the divergent term in Eq. (10) is neglected in this paper. The coefficient  $C$  in Eq. (10) is introduced to adjust density of blackbody radiation to that of light incident on our retina. Specifically, by assuming that one is looking at a surface lit by moonlight, with a color temperature of 4100 K and a luminance  $L \text{ Cd}\cdot\text{m}^{-2}$ , the ratio of the intensity of light falling on the retina over the light falling on the cornea as 0.5, the pupil area  $3.8 \times 10^{-5} \text{ m}^2$ , and the distance from the lens to the retina of 0.0167 m, we obtain  $C = L/4.0 \times 10^{10}$ . Here, a conversion from luminous flux in  $\text{Cd}\cdot\text{sr}$  to radiant flux in  $\text{W}\cdot\text{m}^{-1}$  was done by using the spectral luminous efficiency function for scotopic vision [14].

From Eqs. (8) and (10), we obtain the transition probability in (3) as,

$$w_{ji} = \begin{cases} CB_{ji}W(-\omega_{ji}) + A_{ji} + |Q_{ji}|^2 J(-\omega_{ji}) [\bar{n}(-\omega_{ji}) + 1] & \text{for } \omega_{ji} < 0 \\ CB_{ji}W(\omega_{ji}) + |Q_{ji}|^2 J(\omega_{ji}) \bar{n}(\omega_{ji}) & \text{for } \omega_{ji} > 0 \end{cases}, \quad (11)$$

where  $A_{ij}$  and  $B_{ij}$  are Einstein  $A$  and  $B$  coefficient in between the  $i$ th and  $j$ th eigenstate of  $H_S$ , and  $W(\omega)$  is the Planck's energy density. The dephasing ratio  $\gamma_{ij}$  in (4) is evaluated by numerical integration of Eq. (8).

### III. RESULTS AND DISCUSSION

Figure 1b shows the time propagation of molecular populations under a typical laser pulse of time duration 5 fs, amplitude  $4 \times 10^9$  V/m, and a carrier frequency of  $2 \times 10^4$  cm<sup>-1</sup> that is resonant with the excitation to the electronic excited state around the Franck-Condon region. The transition dipole moment, set at 10 Debye, corresponds to an oscillator strength  $f \approx 1$ . At time  $t = 0$ , the *cis* population  $P_{cis}(t = 0)$  is almost unity, and after  $t = 10$  fs, probability is created in the excited state. Each panel in the Fig. 1b shows the relaxation process with a different degree of system-environment coupling:  $\eta = 12.5, 25$  and 50. Evident is the fact that the *trans* yield is lower, and the isomerization is faster, with increasing coupling  $\eta$  to the bath. We note that the time scale of the reaction in Fig. 1 is in accord with that observed experimentally using coherent light excitation of rhodopsin, i.e. on the order of 200 fs [1, 2].

By contrast, the time dependence of the molecular populations for the case of excitation by incoherent light is shown in Fig. 2. Here we examine the problem in a context relevant to realistic biological systems. As seen in Fig. 2, for all  $\eta$  the rate of increase of  $P_{trans}$  is linear in time after a time that we denote as  $t_c(\eta)$ . Subsequent to that time the slope of  $P_{trans}$  vs.  $t$  is  $s = 9.4 \times 10^{-8}$  s<sup>-1</sup>, corresponding to a *cis/trans* isomerization timescale of



almost one year. Note that the slope  $s$  is independent of the speed of photoisomerization observed under pulsed laser conditions, as evidenced by the fact that it is independent of  $\eta$ . Rather, this rate of transformation is dictated by the photon flux, which is the rate limiting reagent in the process. By contrast, the time  $t_c$ , which corresponds well to the time scale of photoisomerization under the laser pulse, relates directly to  $\eta$  as  $t_c\eta \approx 20$  ps. For example, for the case of  $\eta = 12.5$ ,  $t_c = 1.5$  ps, in accord with Fig. 1b.

Figure 2b shows the time dependence of  $P_{trans}$  as a function of the luminance  $L$  of the incoherent light source. The slope  $s$  is seen to be proportional to the luminance  $L$  as  $s/L \approx 3.1 \times 10^{-6} \text{ Cd}^{-1} \cdot \text{m}^2 \cdot \text{s}^{-1}$ .

Since the isomerization of only a few molecules are necessary to induce hyperpolarization in a rod cell [4], we compute  $P_3$ , the probability that at least three from among all of the *cis* molecules in a rod cell are converted to *trans*. The probability would then correspond to the rate of our initial visual process under moonlight conditions. The probability  $P_3(t)$  that at time  $t$  at least three from among  $N$  molecules are *trans* is given by  $1 - p_0 - p_1 - p_2$ , where

$$p_n = C_N^n p^n (1 - p)^{N-n} \quad (12)$$

is a probability that  $n$  from among  $N$  molecules are converted to *trans*. Here,  $p = P_{trans}(t)$  is the probability that a molecule is *trans* at time  $t$ , and  $C_N^n$  is the binomial coefficient. For the case of vision, we take the number of rhodopsin molecules in a rod cell to be  $N = 4 \times 10^9$  [15], and assume that the time dependence of  $P_{trans}$  maintains a constant slope  $s$  until  $t = 25$  msec. The resultant  $P_3$  values are shown in Fig. 3, where the time scale to obtain at least three

*trans* molecules is on the order of a few tens of milliseconds. This finding is consistent with experimental time scales of 10 msec for dim flash response of a rod cell [4]. We note, as in the previous results, that the speed of photoisomerization under pulsed laser conditions bears no relation to the far longer time scales associated with the evolution of probability  $P_3$ , since the photon flux is rate-determining in the latter case. Note further that the times at which  $P_3(t)$  reaches the value of 0.5, a measure of the biological response, is virtually a linear function of the irradiance.

Thus far, molecular time evolution in incoherent light was considered using the Redfield approach. We also find that the population transfer can be modeled analytically by solving the simple three state model with the four reaction rates shown in Fig. 4. A comparison with the computed Fig. 2 gives excellent results. Here, states  $A$ ,  $B$ , and  $C$  represent *cis*, excited, and *trans* conformations of the molecule, respectively. The values of  $k_2$  and  $k_4$  correspond to rates of population transfer from  $P_e$  to  $P_{cis}$  and  $P_{trans}$ , which are mainly caused by the system–environment coupling. Values obtained from the coherent pulse studies of Fig. 1 give  $k_2 = k_4 = 0.08\eta\text{ps}^{-1}$ . The  $k_1$  and  $k_3$  represent rates of population transfer from  $P_{cis}$  and  $P_{trans}$  to  $P_e$ , caused by both system–environment coupling and photoabsorption. The rates of system–environment coupling can be assigned using detailed balance, and the rates of photoabsorption are given by the Einstein transition probability from the electronic ground state to the electronic excited state. In the case of  $k_1$ , the primary contribution is photoabsorption, giving  $k_1 = BW = L \times 5.6 \times 10^{-6} \text{Cd}^{-1} \cdot \text{m}^2 \cdot \text{s}^{-1}$ , where  $B$  is the Einstein  $B$  coefficient, and  $W$  is density of energy of the radiation field. The densities of the field

used in Fig. 4 correspond to the luminescence values used in Fig. 2 [16]. On the other hand, in the case of  $k_3$ , the dominant term is system–environment coupling, and we obtain  $k_3 = k_4 \times 1.87 \times 10^{-9}$ . With the resultant  $k_1, k_3 \ll k_2, k_4$ , the rate equations give the reaction rate for isomerization under incoherent light as  $k_1/2 = BW/2$ . Further, these equations establish the existence of a linear region for  $P_{trans}$  vs.  $t$  with an  $\eta$  independent slope  $s = k_1/2$  after a time  $t_c = 3/(k_2 + k_4)$ , relating the rate approach to both the computed coherent and incoherent results.

We note that the reaction rate obtained by the three state model is  $\approx 10\%$  smaller than that given by the Redfield equation. The difference mainly comes from the simplifying assumption that  $k_2 = k_4$ , and the evaluation of the rate of photoabsorption at the torsional angle  $\alpha$  set to zero. Nonetheless, all of the trends seen in the Redfield computed results are also evident in the rate equation results.

#### IV. SUMMARY

We have presented a unified theoretical model of photoisomerization under both a coherent light source such as a femtosecond laser pulse and an incoherent light source such as the moonlight. A minimal model of the isomerization process that gives the same timescale as the femtosecond laser experiment was obtained. It was shown that the time scale for photoisomerization under coherent light corresponds to the initial rise time  $t_c$  of the photoisomerization under incoherent light. Further, we introduced a simple three state model that incorporates all of the relevant rates obtained from both the femtosecond and millisecond

time domains.

This approach provides a connection between the time domain of the femtosecond laser experiment and that of biologically relevant response time scales. A dynamical behavior is seen even for the case of incoherent light source, since sudden irradiation of the light at  $t = 0$  introduces partial coherence into the system. The very earliest dynamics correlate with the primary event of isomerization as identified in femtosecond laser experiments. The exact response observed reflects the combined effect of the characteristics of the radiation field and the underlying dynamics.

Acknowledgment: This work was carried out with partial support from Photonics Research Ontario and NSERC Canada. We thank Professor R.J. Dwayne Miller for extensive comments on a earlier version of this manuscript.

- 
- [1] Q. Wang, W. Schoenlein, L. A. Peteanu, R. A. Mathies, and C. V. Shand, *Science* **266**, 422 (1994).
  - [2] H. Kandori, Y. Shichida, and T. Yoshizawa, *Biochemistry(Moscow)* **66**, 1483 (2001).
  - [3] T. Kobayashi, T. Saito, and H. Ohtani, *Nature* **414**, 531 (2001).
  - [4] N. Sperelakis, ed., *Cell Physiology Source Book* (Academic Press, San Diego, 1998), chap. 47, 2nd ed.
  - [5] X.-P. Jiang and P. Brumer, *J. Chem. Phys.* **94**, 5833 (1991).
  - [6] X.-P. Jiang and P. Brumer, *Chem. Phys. Lett.* **180**, 222 (1991).
  - [7] R. G. Redfield, *IBM J. Res. Dev.* **1**, 19 (1957).
  - [8] K. Blum, *Density Matrix Theory and Applications* (Plenum Press, New York, 1981).
  - [9] V. May and O. Kühn, *Charge and Energy Transfer Dynamics in Molecular Systems* (Wiley-VCH, Berlin, 2000).
  - [10] W. T. Pollard, A. K. Felts, and R. A. Friesner, *Adv. Chem. Phys.* **93**, 77 (1996).
  - [11] H. Davison, *Physiology of the Eye* (Macmillan Press, London, 1990), 5th ed.
  - [12] R. Loudon, *The Quantum Theory of Light* (Oxford University Press, 1983), 2nd ed.
  - [13] W. H. Louisell, *Quantum Statistical Properties of Radiation* (John Wiley & Sons, 1990).
  - [14] ISO/CIE 10527 (1991) CIE Standard Colorimetric Observers.
  - [15] C. N. Graymore, ed., *Biochemistry of the Eye* (Academic Press, London, 1970), chap. 9.
  - [16] Here  $W = 2.5 \times 10^{-11} w(\omega) L$ , where the coefficient is estimated by using the radius of pupil, the distance between the lens and a surface, etc.,  $L$  is luminance of the surface in  $\text{Cd}\cdot\text{m}^{-2}$ , and  $w(\omega)$  is the black body energy density at 4100K. Here,  $W$  and  $w(\omega)$  have units of  $\text{Joule}\cdot\text{sec}\cdot\text{m}^{-3}$ .

### Figure Captions

FIG. 1: a) Potential energy surfaces for the two state model for *cis* to *trans* photoisomerization. The solid curve and dotted curve show diabatic potentials  $V_g$  and  $V_e$ , respectively. The dashed curve shows a coupling potential between two diabatic electronic states. b) Time propagation of *cis* and *trans* populations under a short intense pulse for different values of  $\eta$ .  $P_{cis}$  is the population in the range  $-\frac{\pi}{3} \leq \alpha \leq \frac{\pi}{3}$  on  $V_g$ ,  $P_{trans}$  is that in the range  $-\pi \leq \alpha \leq -\frac{2\pi}{3}$  on  $V_e$ , and  $P_e = 1 - P_{cis} - P_{trans}$ . Note that in Panels b and c, the very short time dynamics, which includes the excitation from the *cis*, is not evident due to the short time over which it occurs.

FIG. 2: a) Time dependence of  $P_{trans}$  for three  $\eta$  values with incoherent light luminescence  $L = 0.03 \text{ Cd}\cdot\text{m}^{-2}$ . b) Time dependence of  $P_{trans}$  for various values of  $L$ , with system–environment coupling  $\eta = 25$ . In all cases there is a deviation from strictly linear behavior at the early times that corresponds to timescales of isomerization dynamics.

FIG. 3: Time dependence of the probability  $P_3$  that at least three from among  $4 \times 10^9$  *cis* molecules become *trans* for various values of  $L$ :  $0.060 \text{ Cd}/\text{m}^2$  (solid);  $0.030 \text{ Cd}/\text{m}^2$  (dotted);  $0.015 \text{ Cd}/\text{m}^2$  (dashed).

FIG. 4: a) Three states model with reaction rates  $k_1$ ,  $k_2$ ,  $k_3$ , and  $k_4$ . Time propagation of  $P_C$  for each luminance  $L$  and strength parameter of system–environment coupling  $\eta$ . Compare with results shown in Fig. 2.

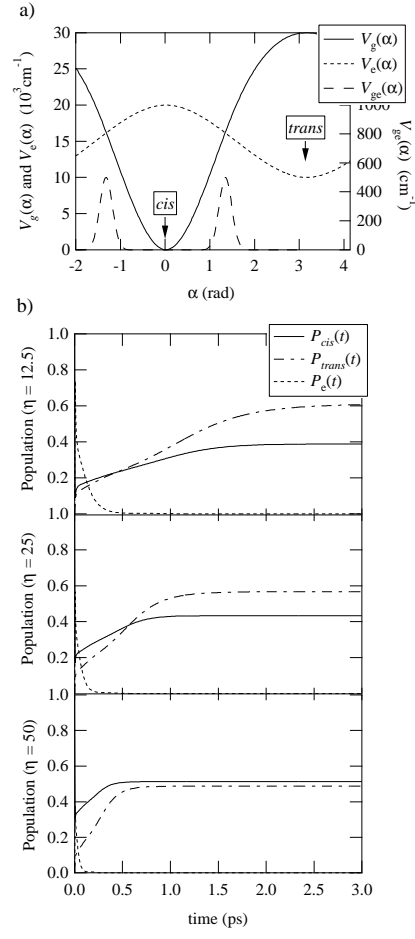


FIG. 1:

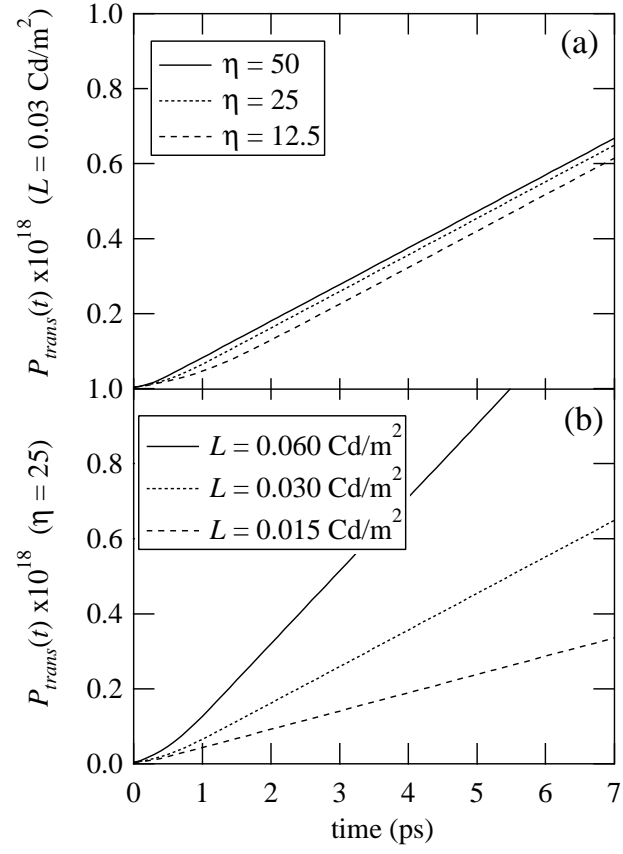


FIG. 2:



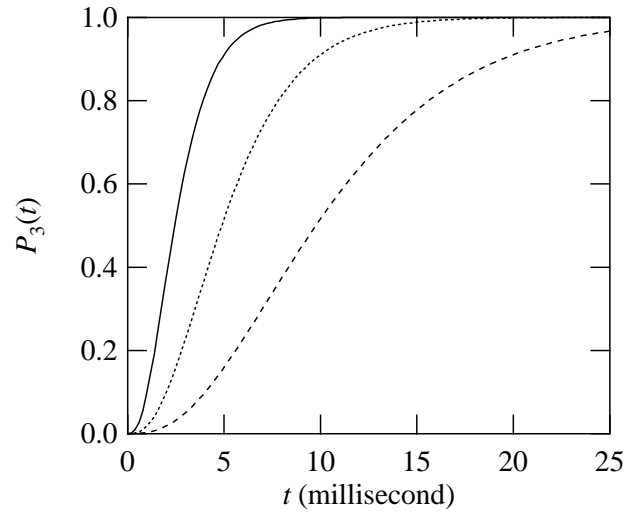
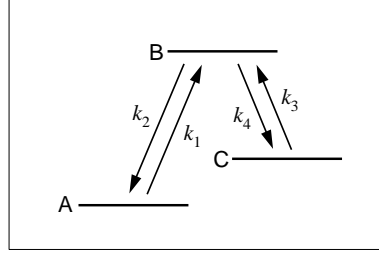


FIG. 3:

a)



b)

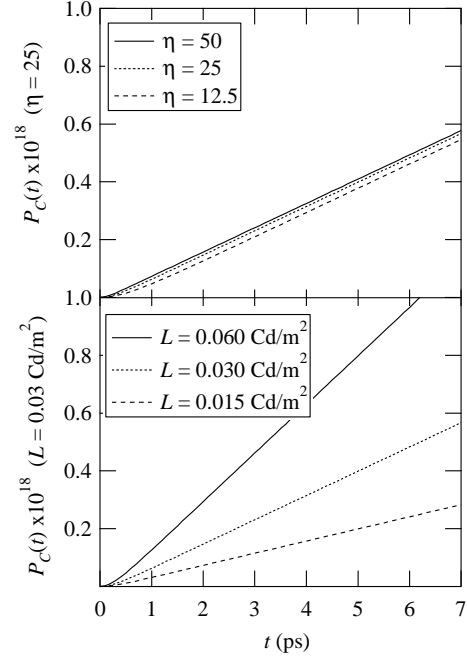


FIG. 4: